

# Deriving Pareto-optimal performance bounds for 1 and 2-relay wireless networks

Qi Wang <sup>\*†‡</sup>, Katia Jaffrès-Runser<sup>†</sup>, Claire Goursaud<sup>‡</sup>, Jun Li<sup>\*</sup>, Yi Sun<sup>\*</sup>, Jean-Marie Gorce<sup>‡</sup>

<sup>\*</sup>Institute of Computing Technology, Chinese Academy of Sciences, Beijing, CHINA

Email: {wangqi08, lijun, sunyi}@ict.ac.cn

<sup>†</sup>Université de Toulouse, IRIT / ENSEEIHT, F-31061, Toulouse, FRANCE

Email: katia.jaffres-runser@irit.fr

<sup>‡</sup>Université de Lyon, INRIA, INSA-Lyon, CITI, F-69621, FRANCE

Email: {claire.goursaud, jean-marie.gorce}@insa-lyon.fr

**Abstract**—This work addresses the problem of deriving fundamental trade-off bounds for a 1-relay and a 2-relay wireless network when multiple performance criteria are of interest. It is based on a MultiObjective (MO) performance evaluation framework composed of a broadcast and interference-limited network model; capacity, delay and energy performance metrics and an associated MO optimization problem. Pareto optimal performance bounds between end-to-end delay and energy for a capacity-achieving network are derived for 1-relay and 2-relay topologies and assessed through simulations. Moreover, we also show in this paper that these bounds are tight since they can be reached by simple practical coding strategies performed by the source and the relays. Two different types of network coding strategies are investigated. Practical performance bounds for both strategies are compared to the theoretical upper bound. Results confirm that the proposed upper bound on delay and energy performance is tight and can be reached with the proposed combined source and network coding strategies.

**Index Terms**—Multiobjective performance evaluation, fundamental bounds, wireless networks, random linear network coding, fountain codes

## I. INTRODUCTION

Two main and complementary directions have driven research in wireless ad hoc networking. The first direction targets the design of efficient distributed protocols at all layers of the protocol stack: physical, medium access control (MAC), routing, and transport layers. The second research direction targets the derivation of fundamental performance limits of wireless ad hoc networks (cf. [1] and the references herein). Both directions are clearly related since performance limits can provide insight into proper network design solutions and thus, help improving protocol performance. They provide as well upper bounds against which to compare the performance of existing protocols.

Initial research in both directions has concentrated on deriving upper bounds [2] and protocols maximizing network capacity [3]. Yet, capacity achieving strategies and related bounds even for some simple network configurations are still to be found [1], [4]. With the introduction of new applications (e.g. wireless sensor networks, vehicular networks, etc...), additional metrics and their impact on network capacity have become relevant. New studies on the trade-off between metrics implying energy consumption minimization [5], [6], end to end

delay minimization [5] or reliability maximization [6] have started. These trade-offs can be characterized with MultiObjective (MO) bounds. A 2-objective MO bound represents the relationship between two criteria  $f_1$  and  $f_2$ . As considered by Goldsmith et al. in [1], a promising way towards achieving fundamental MO bounds in wireless ad hoc networks is to leverage “the broadcast features of wireless transmissions through generalized network coding, including cooperation and relaying”.

In our previous work [7], we have proposed a framework composed of a cross-layer network model to capture the trade-off between reliability, delay and energy metrics for a static wireless ad hoc network. This framework has been designed to incorporate broadcast and interference-limited channels and thus, is capable of deriving MO bounds for a *layerless* communication paradigm. The ad hoc network considered in [7] relies on a directed acyclic graph (DAG) model where all performance metrics (reliability, average end-to-end delay and overall energy consumption) are derived for the set of all possible source-destinations paths when a maximum number of hops is enforced. This last assumption mirrors in the framework of [7] the use of a Time To Live (TTL) flag in the packets transmitted on the DAG.

The purpose of this paper is to lift the DAG and TTL assumption to derive *steady state* network performance metrics (related to reliability, capacity, average end-to-end delay and overall energy consumption). In this new framework, the impact of possibly very long paths may be accounted for in the performance criteria. From this new criteria definition, Pareto-optimal solutions that concurrently optimize all criteria can be extracted, creating more general upper MO performance bounds for given topologies. The framework is illustrated in this work for a 1-relay and 2-relay topology. In the 2-relay topology, solutions where packets can loop between both relays are possible.

The quality of the derived upper MO bounds is assessed through the derivation of achievable lower MO bounds. An achievable lower MO bound can be obtained with any distributed network protocol involving relaying, coding or cooperation decisions at the relays. Our aim is to exhibit the lower achievable MO bounds that are as close as possible to

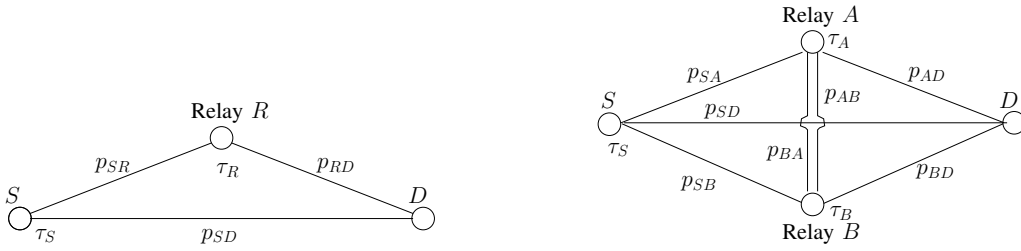


Fig. 1. 1-relay and 2-relay network topologies

our upper MO bound, validating the tightness of the latter and the efficiency of the network strategy. More specifically, this paper investigates lower bounds achieved using source and network coding algorithms. Looking at first for simple transmission and relaying strategies is motivated by their ease of deployment. Focusing on network coding is driven by the fact that it leverages the inherent broadcast nature of wireless propagation, phenomenon that is captured as well in our framework used to derive MO bounds. Results clearly demonstrate the tightness of the analytical upper MO bound to a lower achievable MO bound obtained with a combined source and network coding strategy at the relays. Moreover, for the 2-relay case, we exhibit the benefit of leveraging loops in paths as network coding is performed at the relays: the re-combination of packets along the loop with packets from the source introduces packet diversity and improves the performance criteria trade-offs.

This paper is organized as follows. Section II introduces the underlying network and protocol models where nodes take stochastic forwarding decisions. In Section III, performance evaluation criteria are firstly defined. Next, the MO optimization problem that is solved to derive the MO bounds and sets is introduced. Section IV details the performance criteria for different 1-relay and 2-relay study cases, separating interference-free scenarios from scenarios where interference exists. MO bounds for these study cases are given in Section VI-B and assessed with coding strategies in Section VI. Finally, Section VII concludes the paper.

## II. SYSTEM MODEL

The 1-relay and 2-relay topologies of wireless ad hoc networks, illustrated in Fig. 1 are studied in this paper.

### A. Network and protocol models

We assume a synchronized wireless ad hoc network where transmissions are time-multiplexed (the synchronization procedure is out of the scope of this paper). A frame of  $|\mathcal{T}|$  time slots is repeated indefinitely. In the rest of this paper, our examples assume that one packet is being sent in one time slot.

1) *Wireless channel model*: For any time slot  $u \in \mathcal{T}$ , there is an interference-limited channel between any two nodes  $i$  and  $j$  of the network. This channel is modeled by the probability of a packet to be correctly transmitted between  $i$  and  $j$  in time slot  $u$ . This probability is referred to as the *channel probability*

$p_{ij}^u$  and computed assuming interference is modeled as an additive noise and for the medium access scheme presented hereafter. Its derivation is based on the distribution of the packet error rates (PER) [7] originating from the statistics of nodes attempting emission in the same time slot.

Each channel is assumed to be in a half-duplex mode, i.e. a node cannot transmit and receive a packet at the same time.

2) *Network model*: The considered 1-relay and 2-relay wireless networks are modeled by a finite weighted multiple edges complete graph  $\mathcal{K}_{|\mathcal{V}|} = (\mathcal{V}, \mathcal{E})$  with  $\mathcal{V}$  the set of vertices and  $\mathcal{E}$  the set of edges. An edge  $(i, j, u)$  represents the channel between nodes  $i$  and  $j$  in time slot  $u$ . Each edge is assigned a weight of  $p_{ij}^u$ .

### B. Medium access control for broadcast transmissions

We assume a very basic random channel access for all nodes sharing a time slot  $u$ : if a node  $i$  is willing to transmit its packet in time slot  $u$  in the next frame, it attempts emission with probability  $\tau_i^u$  and disregards the packet with probability  $1 - \tau_i^u$ . There is no acknowledgment procedure. Contrary to more elaborated medium access procedures, emission decisions are independent.

The *emission rate*  $\tau_i^u$  is defined as the probability node  $i$  is emitting in time slot  $u$ . A particular instance of  $\tau$  values is *feasible* if and only if the following Properties 1 and 2 hold:

**PROPERTY 1: Flow conservation.** The sum rate of all outgoing links is lower or equal to the sum rate of all incoming links.

**PROPERTY 2: Half duplex.** A node  $j$  is able to receive a message on a time slot  $u$  if it is not transmitting on that same time slot. Thus, a  $\tau$  is feasible if for each node of the network, the average number of time slots it spends transmitting and receiving sums up to a maximum value of one.

We define a set of *active emissions*  $\mathcal{A}$  corresponding to the values of  $\tau$ . An emission  $(i, u) \in \mathcal{V} \times \mathcal{T}$  is said to be active if  $\tau_i^u > 0$ . As a consequence, the set  $\mathcal{A}$  is given by  $\mathcal{A} = \{(i, u) \in \mathcal{V} \times \mathcal{T} \mid \tau_i^u > 0\}$ . We define  $\Gamma$  as the set of all feasible emission rate matrices.

### C. Forwarding and scheduling decisions

Each node  $j$  will decide, with the *forwarding probability*  $x_{ij}^{uv}$ , to transmit on time slot  $v$  a packet coming from node  $i$  in the time slot  $u$  of the next frame. All forwarding probabilities are grouped in a matrix  $X \in \mathcal{X}$  with  $\mathcal{X}$  the set of all matrices.

The forwarding probabilities is related to the emission rates and channel probabilities with the following set of  $|\mathcal{A}|$  equations

$$\sum_{(i,j) \in \overline{\mathcal{N}}_j^i} \sum_{u \in \mathcal{T}} \tau_i^u p_{ij}^u x_{ij}^{uv} = \tau_j^v, \quad \forall (j,v) \in \mathcal{A} \quad (1)$$

where  $\tau_i^u p_{ij}^u$  is the probability that a packet sent by  $i$  on time slot  $u$  arrives in  $j$ . These equations ensure that for each active emission, the forwarding decisions applied to the incoming flows create the appropriate emission rate  $\tau_j^v$ . We define  $\mathcal{X}^\tau$  as the set of forwarding matrices verifying (1).

The forwarding probabilities represent the decisions of the nodes to either (i) retransmit all the packets received or (ii) reduce the output rate by dropping or re-encoding them. The algorithm describing the forwarding and transmission decisions taken by a relay node is given in Algorithm 1.

---

**Algorithm 1** Relay algorithm

---

```

for each time slot  $u$  do
  if  $u \neq v$  then
    if Relay  $j$  receives a packet  $p$  from  $i$  in slot  $u$  then
      Generate a random value  $x \in [0, 1]$ ;
      if forwarding decision  $x_{ij}^{uv} \geq x$  then
        Store the packet  $p$  into FIFO memory of size  $B$ 
      else
        Drop  $p$ 
      end if
    end if
  else
    if FIFO is not empty then
      Transmit the packet  $p$  in time slot  $v$ ;
    end if
  end if
end for

```

---

### III. MO OPTIMIZATION PROBLEM

#### A. Elementary criteria definition

This section defines, for one source-destination flow, optimization objectives related to capacity, reliability, end-to-end delay and energy consumption based on the aforementioned network and protocol model.

**CAPACITY OBJECTIVE  $f_C$ :** It is defined as the average number of packets received by destination  $D$  per packet sent by source  $S$ . If  $\mathcal{P}$  is the set of all possible paths on  $\mathcal{K}_{|V|}$  between  $S$  and  $D$ , it is derived by summing the transmission success probability of a packet on each path. Formally:

$$f_C = \sum_{\mathbf{p} \in \mathcal{P}} P(\mathbf{p}) \quad (2)$$

where  $P(\mathbf{p})$  is the transmission success probability of a packet on path  $\mathbf{p} \in \mathcal{P}$ .

**RELIABILITY OBJECTIVE  $f_R$ :** It is defined as the probability of a packet to arrive at  $D$ . It is equivalent to the success rate of a packet sent by the source. It differs from the capacity

criterion because redundant packet copies that successfully arrive at  $D$  are not accounted for. More specifically, it is the probability that at most one copy arrives at  $D$ . Formally:

$$f_R = 1 - \prod_{\mathbf{p} \in \mathcal{P}} (1 - P(\mathbf{p})) \quad (3)$$

**DELAY OBJECTIVE  $f_D$ :** It is defined as the average delay a packet sent by the source needs to reach the destination, expressed in number of hops. Assuming that one hop introduces a delay of 1 unit, a  $h$ -hop transmission introduces a delay of  $h$  units. Having  $H(\mathbf{p})$  the length in hops of path  $\mathbf{p}$ , the average end-to-end delay is computed by:

$$f_D = \frac{\sum_{\mathbf{p} \in \mathcal{P}} H(\mathbf{p}) \cdot P(\mathbf{p})}{\sum_{\mathbf{p} \in \mathcal{P}} P(\mathbf{p})} = \frac{\sum_{\mathbf{p} \in \mathcal{P}} H(\mathbf{p}) \cdot P(\mathbf{p})}{f_C} \quad (4)$$

where the numerator provides the total delay of all paths and the denominator the number of copies received, in average.

**ENERGY OBJECTIVE  $f_E$ :** We consider as a first approximation that the main energy consumption factor is due to the emission of a packet. Thus, the energy criterion  $f_E$  is defined as the average number of emissions performed by all nodes (source and relays) per packet sent by the source.

#### B. Capacity and reliability achieving criteria

We define as well two other types of criteria, naming *reliability achieving* and *capacity achieving* criteria. These objectives directly derive from the elementary objectives introduced earlier.

**RELIABILITY ACHIEVING DELAY  $f_D^r$  AND ENERGY  $f_E^r$ :**

$$f_D^r = f_D / f_R \quad (5)$$

$$f_E^r = f_E / f_R \quad (6)$$

They represent the delay and energy needed to reach a perfectly reliable transmission.

**CAPACITY ACHIEVING DELAY  $f_D^c$  AND ENERGY  $f_E^c$ :**

$$f_D^c = f_D / \min(f_C, 1) \quad (7)$$

$$f_E^c = f_E / \min(f_C, 1) \quad (8)$$

Here, capacity achieving criteria  $f_D^c$  and  $f_E^c$  are obtained by dividing the value of  $f_D$  and  $f_E$  by  $\min(f_C, 1)$  respectively.

Capacity and reliability criteria are equal if the packet travels on a unique path between  $S$  and  $D$ . When more than one path connect  $S$  and  $D$ , these criteria may not be equal anymore because several copies may reach  $D$ . More generally,  $f_C$  upper bounds reliability:  $f_C \geq f_R$ .

#### C. MO Optimization problem

In our MO problem, we optimize the location  $l \in \mathcal{C}$  of the  $N$  relays, chosen in the convex set  $\mathcal{C}$ , and their forwarding probabilities represented by  $X \in \mathcal{X}^\tau$ . Each solution  $X \in \mathcal{X}^\tau$  can be evaluated according to  $f_C, f_D$  or  $f_E$ . In this paper, the following multiobjective optimization problem is solved:

$$\begin{aligned} & [\min f_D^c(x), \min f_E^c(x)]^T \\ \text{s.t.} \quad & x = (l, \tau, X) \in \mathcal{C}^N \times \Gamma \times \mathcal{X}^\tau \end{aligned} \quad (9)$$

#### D. Multiobjective performance bounds

In this work, we define a Pareto-optimal capacity-achieving upper bound  $\mathcal{B}_{opt}^c$  and a Pareto-optimal reliability-achieving lower bound  $\mathcal{B}_{opt}^r$ .

- The  $\mathcal{B}_{opt}^c$  upper bound is given by:

$$\mathcal{B}_{opt}^c = \{(f_D^c(x), f_E^c(x)) \mid \forall x \in \mathcal{S}_{opt}\}$$

This bound and  $\mathcal{S}_{opt}$  are obtained by solving (9), with  $\mathcal{S}_{opt}$  the set of Pareto-optimal solutions.

- The  $\mathcal{B}_{opt}^r$  lower bound is given by:

$$\mathcal{B}_{opt}^r = \{(f_D^r(x), f_E^r(x)) \mid \forall x \in \mathcal{S}_{opt}\}$$

$\mathcal{B}_{opt}^r$  is computed once the Pareto-optimal solutions are obtained by solving (9). Each Pareto-optimal solution of  $\mathcal{S}_{opt}$  is analyzed by simulations.  $\mathcal{B}_{opt}^c$  is an upper bound: it represents the ideal case where all packets received at each destination are linearly independent. On the opposite,  $\mathcal{B}_{opt}^r$  is a lower realistic bound where identical packets are received if more than one path connects  $S$  and  $D$ . These bounds are equal if  $f_R = f_C$ . That may happen when the packet travels on a unique path between  $S$  and  $D$  or optimal coding solutions are found.

#### IV. BOUNDS FOR 1-RELAY AND 2-RELAY TOPOLOGIES

##### A. Study cases

For the two topologies presented in Fig. 1, six different study cases are considered and summarized in Table I. In all study cases, the source only emits packets on the first time slot with rate one:  $\tau_S^1 = 1$  and  $\forall u \neq 1, \tau_S^u = 0$  and destination only receive packets. We assume that each relay has a buffer of size  $B$ . In general, a relay  $j$  receiving a packet coming from node  $i$  in the time slot  $u$  has to decide whether to forward it or not on time slot  $v$  according to the forwarding probability  $x_{ij}^{uv}$  as mentioned in section II-C. If the relay  $j$  decides to forward the packet, it will store it in its incoming buffer and transmit it in time slot  $v$  as shown in Algorithm 1.

Each study case defines which topology is assumed, how many time slots constitute a frame and which nodes are allowed to transmit in each time slot. The time slot assignments of study cases 1, 3 and 4 ensure no interference exists, while other study cases exhibit time slots with possible interference. The forwarding probabilities can be chosen in study cases 4 and 6 such as loops between relays  $A$  and  $B$  may exist, while for study cases 3 and 5, constraints enforce that no loop exists. For each study case, section IV-B defines the related MO optimization problem solved.

##### B. Criteria for 1-relay and 2-relay topologies

For both topologies, the general multiobjective problem of (9) is considered. Expressions are detailed as follows:

1) *1-relay topology*: For a 1-relay topology using  $|\mathcal{T}|$  time slots, optimization objectives are defined as:

$$f_C = \tau_S^1 p_{SD}^1 + \sum_{u=1}^{|\mathcal{T}|} \tau_S^u p_{SR}^u x_{SR}^{1u} p_{RD}^u \quad (10)$$

$$f_R = 1 - (1 - \tau_S^1 p_{SD}^1) \prod_{u=1}^{|\mathcal{T}|} (1 - \tau_S^u p_{SR}^u x_{SR}^{1u} p_{RD}^u) \quad (11)$$

$$f_D = (\sum_{u=1}^{|\mathcal{T}|} 2 \cdot \tau_S^u p_{SR}^u x_{SR}^{1u} p_{RD}^u + \tau_S^1 p_{SD}^1) / f_C \quad (12)$$

$$f_E = \tau_S^1 + \sum_{u=1}^{|\mathcal{T}|} \tau_S^u p_{SR}^u x_{SR}^{1u} \quad (13)$$

TABLE I  
STUDY CASES

Study case	Topology	$ \mathcal{T} $	Nodes transmitting on slot			Loop between A and B
			1	2	3	
1	1-Relay	2	$S$	$R$	-	-
2	1-Relay	1	$S, R$	-	-	-
3	2-Relay	3	$S$	$A$	$B$	No
4	2-Relay	3	$S$	$A$	$B$	Yes
5	2-Relay	2	$S$	$A, B$	-	No
6	2-Relay	2	$S$	$A, B$	-	Yes

Study cases 1 and 2 are covered by the MO problem of (9) and objectives are given in Eq. (10) to (13). For **study case 1**,  $|\mathcal{T}| = 2$  time slots,  $S$  emits in time slot 1 and relay  $R$  in time slot 2. Thus, following (1),  $x_{SR}^{11} = 0$  and  $x_{SR}^{12} = \tau_R^2 / (\tau_S^1 p_{SR}^1)$ . As such, the only variables in this problem are the location of the relay  $l_R \in \mathcal{C}$  and its forwarding probability  $x_{SR}^{12} \in [0, 1]$ .

For **study case 2**, since there is only one time slot, a single variable  $x_{SR}^{11}$  is defined. It is directly related to  $\tau_R^1$  following (1):  $x_{SR}^{11} = \tau_R^1 / (\tau_S^1 p_{SR}^1)$ . As such, the only variables in this problem are  $l_R \in \mathcal{C}$  and  $x_{SR}^{11} \in [0, 1]$ .

2) *2-relay topology*: For the interference free study cases 3 and 4, we have  $|\mathcal{T}| = 3$  time slots.  $S$  transmits in time slot 1 while relays  $A$  and  $B$  transmit in time slot 2 and 3, respectively. Consequently, only  $\tau_A^2$  and  $\tau_B^3$  are defined, other relay emission rates are set to 0. For **study case 3**, only  $x_{SA}^{12}$ ,  $x_{SB}^{13}$  are non zero variables. The criteria can be easily derived from (10) to (13) by adding the contribution introduced by another relay node. For **study case 4**, different from study case 3,  $x_{BA}^{32}$  and  $x_{AB}^{23}$  are non zero variables as well. Moreover, an  $X \in \mathcal{X}$  matrix is feasible if the 2 constraints from (1) are met:

$$\begin{aligned} \tau_S^1 p_{SA}^1 x_{SA}^{12} + \tau_B^3 p_{BA}^3 x_{BA}^{32} &= \tau_A^2 \\ \tau_S^1 p_{SB}^1 x_{SB}^{13} + \tau_A^2 p_{AB}^2 x_{AB}^{23} &= \tau_B^3 \end{aligned}$$

Introducing the notation  $Q_{ij}^{uv} = p_{ij}^u x_{ij}^{uv}$  and following the derivation in the Appendix, the optimization objectives are :

$$f_C = \tau_S^1 p_{SD}^1 + \frac{\tau_S^1}{1 - Q_{AB}^{23} Q_{BA}^{32}} (E + F) \quad (14)$$

with  $E = (Q_{SA}^{12} + Q_{SB}^{13} Q_{BA}^{32}) p_{AD}^2$  and  $F = (Q_{SB}^{13} + Q_{SA}^{12} Q_{AB}^{23}) p_{BD}^3$ .

$$f_D = \frac{1}{f_C} \cdot \left[ \frac{\tau_S^1}{(1 - Q_{AB}^{23} Q_{BA}^{32})^2} (A + B) + \tau_S^1 p_{SD}^1 \right] \quad (15)$$

with  $A = p_{AD}^2 [Q_{SB}^{13} Q_{BA}^{32} (3 - Q_{AB}^{23} Q_{BA}^{32}) + 2Q_{SA}^{12}]$  and  $B = p_{BD}^3 [Q_{SA}^{12} Q_{AB}^{23} (3 - Q_{AB}^{23} Q_{BA}^{32}) + 2Q_{SB}^{13}]$ .

$$f_E = \tau_S^1 + \frac{\tau_S^1}{1 - Q_{AB}^{23} Q_{BA}^{32}} (Q_{SA}^{12} + Q_{SB}^{13} Q_{BA}^{32} + Q_{SA}^{12} Q_{AB}^{23} + Q_{SB}^{13}) \quad (16)$$

$Q_{AB}^{23} Q_{BA}^{32}$  may be equal to one. As such, we add the following constraint to the MO problem of (9) for study case 4:

$$\forall X \in \mathcal{X} \text{ if } (p_{AB}^2 = 1 \wedge p_{BA}^3 = 1) \left\{ \begin{array}{l} x_{AB}^{23} < 1 - \Delta \\ x_{BA}^{32} < 1 - \Delta \end{array} \right.$$

with an empirically chosen value of  $\Delta = 0.05$ .

For study cases 3 and 5, only one-hop and two-hop transmissions are possible (no loop between two relays). Thus, it is possible as well to derive a closed form expression for  $f_R$ :

$$f_R = 1 - (1 - \tau_{SD}^1 p_{SD}^1)(1 - \tau_{SA}^1 p_{SA}^1 x_{SA}^{1u} p_{AD}^u) \times (1 - \tau_{SB}^1 p_{SB}^1 x_{SB}^{1v} p_{BD}^v) \quad (17)$$

where  $u = 2, v = 3$  for study case 3 and  $u = v = 2$  for study case 5 respectively. For study cases 4 and 6, it is not possible to derive a closed form expression of  $f_R$  because of the loop between  $A$  and  $B$ .

**Study cases 5 and 6** differ from 3 and 4 respectively, since  $A$  and  $B$  emit on the same slot 2. As such, aforementioned criteria are straightforward to adapt to time slot assignment.

## V. RESULTS

The first goal of this paper is to derive the Pareto-optimal upper bounds  $\mathcal{B}_{opt}^c$  and corresponding Pareto-optimal solutions  $\mathcal{S}_{opt}$  for a 1-relay and a 2-relay wireless network. In this section, firstly,  $\mathcal{B}_{opt}^c$  and the set  $\mathcal{S}_{opt}$  are derived from MO optimization as in section III-C. Secondly, the solutions of the analytical upper bounds  $\mathcal{B}_{opt}^c$  are verified by simulations and compared to the lower bounds  $\tilde{\mathcal{B}}_{opt}^r$  obtained when the protocol of Algorithm 1 is simulated with the event-driven network simulator WSNNet [8].

### A. Implementation

For all study cases, the distance between  $S$  and  $D$  is set to  $d_{SD} = 620m$  such as no direct transmission is possible ( $p_{SD}^1 \approx 0$  assuming a transmission power  $P_T = 0.15mW$  and a pathloss exponent of 3). The set of Pareto optimal locations of relays is searched in a continuous square surface area  $\mathcal{C}$  of size  $d_{SD} \times d_{SD}$  meters.

1) *MO optimization*: The upper bound  $\mathcal{B}_{opt}^c$  and  $\mathcal{S}_{opt}$  are obtained using the state of the art non-dominated sorting genetic algorithm (NSGA-2) [9]. For NSGA-2, a population size of 300 solutions is used and a maximum number of 1000 generations. The crossover probability is set to 0.9.

2) *Simulations settings*: Each upper Pareto bound solution is simulated with WSNNet. For each solution, the location of the relays and their forwarding probabilities are known. In our simulations, a perfect TDMA is implemented following the specifications of the study cases.  $S$  sends a packet every first time slot of every frame. Experiment runs for 10000 frames.

Simulated values  $\tilde{f}_C, \tilde{f}_D, \tilde{f}_E, \tilde{f}_D^c$  and  $\tilde{f}_E^c$  are calculated from simulations as follows.  $\tilde{f}_C$  is measured by the total number of packets  $N_{rx}$  received at  $D$  (including copies) divided by the number of packets transmitted by  $S$ .  $\tilde{f}_D$  is measured using the statistical distribution of the delays of the packets arrived over each possible distance measured in hops:  $P(h) = n(h)/N_{rx}$ , where  $n(h)$  is the number of packets arrived in  $h$  hops at  $D$ .  $\tilde{f}_D$  is then calculated with  $\tilde{f}_D = \sum_{h=1}^{h_{max}} h \cdot P(h)$ , with  $h_{max}$  the maximum number of hops of all packets collected at  $D$ .  $\tilde{f}_E$  is the sum of the number of packets transmitted by the source and the relays divided by the number of packets sent by  $S$ . Then, the simulated *capacity-achieving* delay  $\tilde{f}_D^c = \tilde{f}_D / \min(\tilde{f}_C, 1)$  and energy

TABLE II  
THE RMSE FOR STUDY CASES

Study Cases	$\tilde{f}_C$	$\tilde{f}_D$	$\tilde{f}_E$
Study case 1	1.7e-03	0	1.8e-05
Study case 3	1.6e-04	0	2.1e-05
Study case 4	5.2e-04	1.1e-03	2.2e-04
Study case 5	2.6e-04	0	1.8e-05
Study case 6	1.3e-03	2.5e-04	2.5e-02

$\tilde{f}_E^c = \tilde{f}_E / \min(\tilde{f}_C, 1)$  are derived. From that, the empirical version of the upper bound  $\tilde{\mathcal{B}}_{opt}^c$  can be derived.

Besides, for each study case we compute empirically the reliability objective  $f_R$ . It measures the proportion of different packets arriving at  $D$ . It is a regular success rate (copies are disregarded). From  $\tilde{f}_R$ , empirical *reliability-achieving* delay  $\tilde{f}_D^r = \tilde{f}_D / \tilde{f}_R$  and energy  $\tilde{f}_E^r = \tilde{f}_E / \tilde{f}_R$  objectives are defined. From that, the empirical lower bound  $\tilde{\mathcal{B}}_{opt}^r$  can be derived.

### B. Results for considered topologies

A first important conclusion is that in all figures, the analytical bounds and their simulated counterparts perfectly match, assessing our network model and criteria definitions. Table II gives the root mean square error (RMSE) between  $\mathcal{B}_{opt}^c$  and  $\tilde{\mathcal{B}}_{opt}^c$  for all study cases.  $RMSE = \frac{1}{N_{opt}} \sqrt{\sum_{i=1}^N \frac{(f(i) - \tilde{f}(i))^2}{f(i)^2}}$  where  $N_{opt}$  is the total number of Pareto-optimal solutions in  $\mathcal{B}_{opt}^c$ . Values are really small, showing a quasi-perfect match between the model and simulations.

**STUDY CASE 1**: No interference exists in this scenario. Fig. 2(a) shows  $\mathcal{B}_{opt}^c$  and  $\tilde{\mathcal{B}}_{opt}^r$ . Since all packets arriving at  $D$  use the  $S - R - D$  path,  $f_R$  and  $f_C$  are equal, meaning there are no duplicated packets. These solutions have  $x_{SR}^{12} = 1$  and the relay is located in the very close neighborhood of the center of the  $[S, D]$  segment.

**STUDY CASE 2**: Transmissions are interference limited. When  $p_{SD}^1 \approx 0$ , no relay position ensures  $p_{SR} \neq 0$  and  $p_{RD} \neq 0$  simultaneously, thus no solution exists in this case. It is a direct consequence of interference between  $S$  and  $R$ .

**STUDY CASE 3**: As shown in Fig. 2(b),  $\mathcal{B}_{opt}^c$  and  $\tilde{\mathcal{B}}_{opt}^r$  don't coincide because packets can arrive from two different paths. There is a single Pareto-optimal point  $f_D^c = 3.93$  and  $f_E^c = 3.93$ . It is obtained for  $f_C = 0.508351$ . This solution has  $x_{SA}^{12} = 1$  and  $x_{SB}^{13} = 1$  and relays are located exactly in the middle of  $[S, D]$ .

**STUDY CASE 4**: Seen from Fig. 2(c), as expected,  $\mathcal{B}_{opt}^c$  and  $\tilde{\mathcal{B}}_{opt}^r$  are disjoint since multiple copies are received due to the loop between  $A$  and  $B$ . The optimal solutions are obtained for  $f_C \approx 1$ . For these solutions, one relay is in the middle of  $[S, D]$  and the other relay is close to  $D$ , having  $p_{SB}^1 = 0$  and  $p_{BD}^2 = 1$ . The two relays are close together, inducing a perfect link between them with a forwarding probability adjusted to obtain  $f_C \approx 1$ .

**STUDY CASE 5**: The Pareto optimal bound  $\mathcal{B}_{opt}^c$  and  $\tilde{\mathcal{B}}_{opt}^r$  are the same as the bound of study case 1 as shown in Fig. 2(a). Interference between the relays is clearly detrimental to the network performance since solutions with a single relay dominate solutions with two relays.

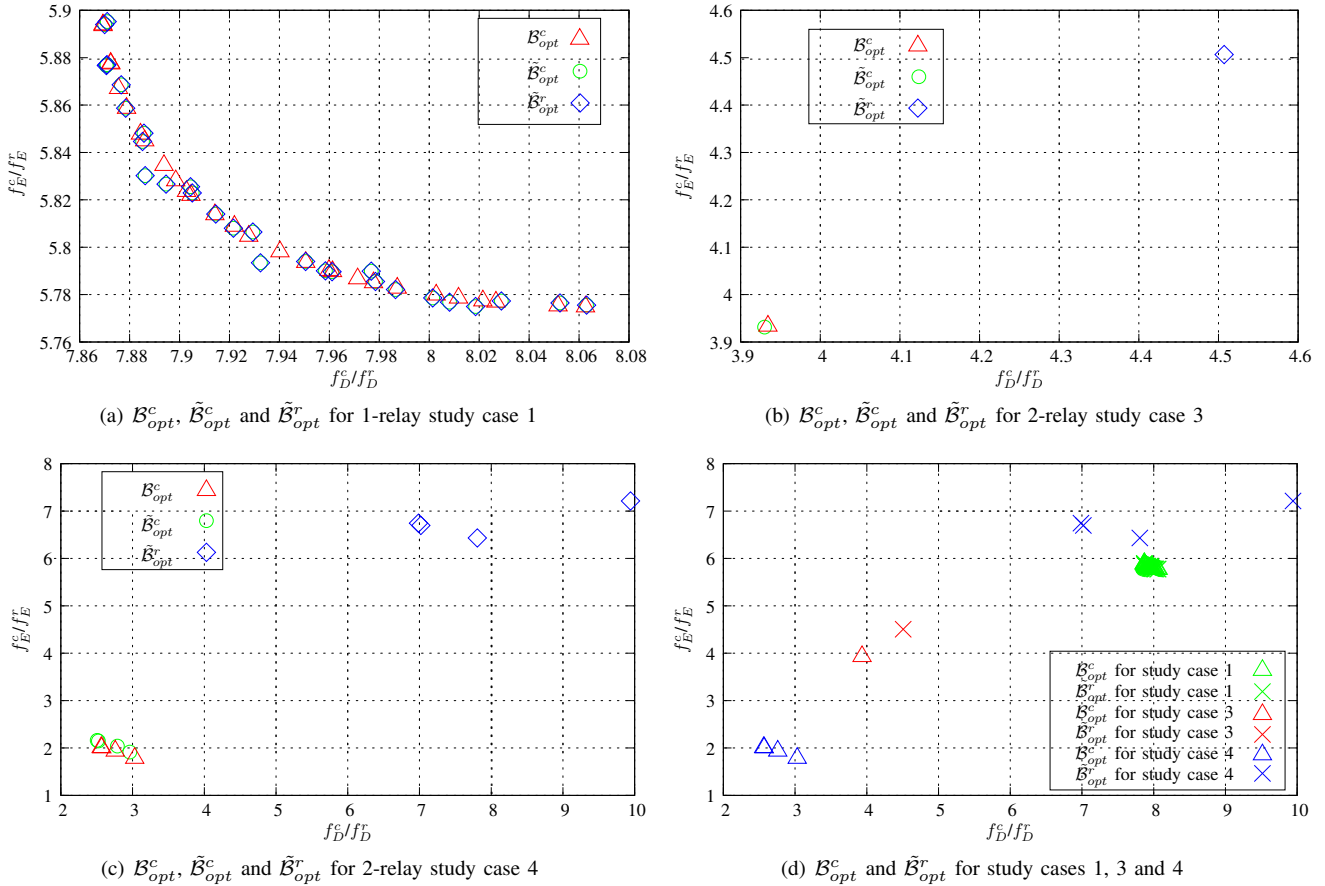


Fig. 2. MO upper and lower bounds for considered network topologies and study cases

**STUDY CASE 6:** Similar to the study case 5, the Pareto optimal bound  $\mathcal{B}_{opt}^c$  and  $\tilde{\mathcal{B}}_{opt}^r$  are same as the study case 1 seen in Fig. 2(a) due to the interference.

### C. COMPARATIVE ANALYSIS

We have studied different study cases and we aim at comparing their performance. First, we have seen that optimizing the problem where the two relays use the same channel in study case 5 and 6 converges to a bound where only one relay is active. Thus, interference limited solutions are, not surprisingly, dominated by interference free solutions. The conclusion is that for bigger networks, optimizing their performance should be done in two steps. First, derive an interference free channel allocation if possible and second, optimize the node's forwarding decisions.

We compare the optimal upper and lower bounds  $\mathcal{B}_{opt}^c$  and  $\tilde{\mathcal{B}}_{opt}^r$  obtained for the interference-free study cases 1, 3 and 4 in Fig. 2(d). Looking at the  $\tilde{\mathcal{B}}_{opt}^r$  bound, better performance is obtained if two relays are used since the  $\tilde{\mathcal{B}}_{opt}^r$  for study case 3 dominates the bound for study case 1. More reliable transmissions are obtained when two relays can be leveraged using our broadcast forwarding mode.

It is really interesting to look at  $\mathcal{B}_{opt}^c$  for study case 4. Study case 4 is the only one where a loop exists between  $A$  and  $B$  in the network. For this case, lots of copies of the same

packet arrive at  $D$  because of the loop. So if it is possible to leverage all these copies using network coding, the network performance can be greatly improved since  $\mathcal{B}_{opt}^c$  dominates the bounds of all other study cases.

If a network coding strategy provides a lower bound performance that reaches  $\mathcal{B}_{opt}^c$ , then the optimization of the network forwarding probabilities can be simplified. There is no need to introduce constraints that avoid the presence of loops in the network. With such a broadcast oriented forwarding mechanism, loops could even become beneficial for network performance since the  $\mathcal{B}_{opt}^c$  of study case 4 clearly outperforms all other lower bounds. In the next section, a simple two-layered coding approach is introduced to show that its efficiency reaches  $\mathcal{B}_{opt}^c$  for study case 4.

### VI. TWO-LAYERED CODING SOLUTION TO REACH $\mathcal{B}_{opt}^c$

The second goal of this paper is to assess the quality of  $\mathcal{B}_{opt}^c$  through the derivation of a lower achievable MO bound with coding. Therefore, in this section, we show how it is possible to breach the gap between  $\mathcal{B}_{opt}^c$  and  $\tilde{\mathcal{B}}_{opt}^r$  for study case 4. The strategy we propose to leverage the redundant packets in the transmission relies on two design strategies:

- the use of fountain codes to ensure end-to-end reliability,
- the use of network coding to introduce packet diversity.

## A. Coding solution

1) *Fountain Codes*: Fountain codes are rateless erasure codes in the sense that a potentially limitless sequence of encoded packets can be generated from the information source. This flow is stopped by the destination when it has received enough packets to recover the information [10]. The major advantage of fountain codes is that they are not channel-dependent, thus the same coded information flow is inherently adapted to any channel type. In this paper, we consider the random linear fountain code (RL code) [10] and Maximum Likelihood decoding (ML-decoding) for the decoding.

2) *Network coding strategies*: Network coding is a technique which consists in combining packets in the node's buffer using exclusive-OR (XOR) operator. This introduces packet diversity at the destination as the received packets are more likely to be independent [11]. We show in the following that the increase in packet diversity induced by network coding is an efficient mean to distributively reach the upper bound  $\mathcal{B}_{opt}^c$ . The different network coding strategies are investigated:

CODING STRATEGY "R-XOR": the  $R$  lastly received packets are XORed together [11], thus the buffer size is  $B = R$ .

CODING STRATEGY "RLNC": A binary Random Linear Network Code (RLNC over  $F_2$ ) [12] is considered. For each packet in the buffer, the relay flips a coin to know whether to add it or not in  $p_{out}$ . A memory of the size  $B = K$  of the RL code dimension is assumed.

## B. Lower bounds with coding

1) *Coding simulations setup*: We consider a message divided into  $K$  fragments whose length is the size of a packet. Transmissions are time multiplexed as well and it takes one time slot to transmit a packet.  $S$  sends one RL encoded packet in the first time slot of each frame. Location of the relays and their forwarding probability from  $\mathcal{B}_{opt}^c$  are used.  $S$  ends the transmission of RL packets as soon as  $D$  can recover the original message and acknowledge the successful reception. Reliability-achieving delay and energy is consistent with the implementation of Section V-A.

The distance between two bounds is measured using the Generational Distance (GD) metric defined as:  $GD = \frac{1}{N_{opt}} \left( \sum_{i=1}^{N_{opt}} (d_i^p) \right)^{1/p}$  with  $d_i$  the Euclidian distance between upper MO bound and lower achievable MO bounds with coding. We use  $p = 2$ . The smaller this metric is, the closer the solutions of lower and upper bounds are from each other.

2) *Coding overheads*: Coding introduces two types of overhead we account for in our study. The first type of overhead is composed of the additional packets needed to decode the encoded stream. This *decoding overhead* is measured by the percentage of packets received in excess compared to the  $K$  initial fragments. Formally, it is equal to  $(N_r - K) * 100/K$  with  $N_r$  is number of packets received at  $D$  before decoding the initial  $K$  fragments.

The second type of overhead results from the transmission of the coding coefficients in encoded packets' header. In this paper, we consider that coefficients are coded over  $K$  bits and

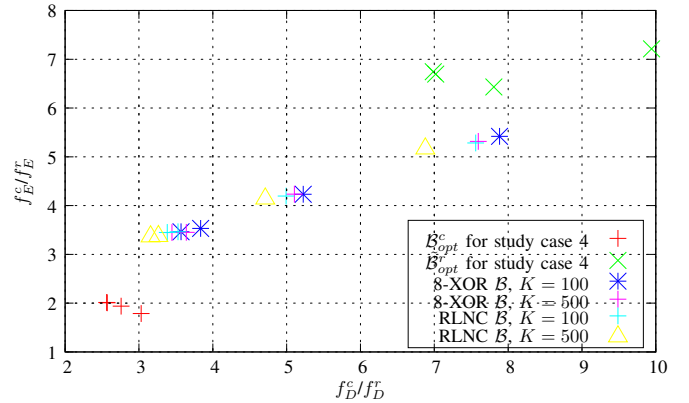


Fig. 3. NC bounds for 2-relay study case 4

TABLE III  
GD AND DECODING OVERHEAD FOR DIFFERENT CODING STRATEGIES

Study Cases	Coding Strategies	GD	Overhead (%)
Study case 4	8-XOR, K=100	1.85	57.6
	8-XOR, K=500	1.77	55.7
	RLNC, K=100	1.74	56.2
	RLNC, K=500	1.57	55.7

that the packet length  $PL$  is 2560 bytes. Thus this *coefficient overhead* is given by  $(PL - K/8)/PL$  and introduced into empirical delay and energy metrics to scale their values.

## C. Lower bound results

Figure 3 shows the lower achievable MO bounds  $\mathcal{B}$  obtained by "R-XOR" and "RLNC" strategies for  $K = 100$  and  $K = 500$ . They are greatly improved than lower bound  $\tilde{\mathcal{B}}_{opt}^r$  if network coding is implemented. Note that this improvement is obtained at the cost of a bigger buffer at the relays. Seen from Table III, the best coding strategy is when adopting the "RLNC" for  $K = 500$  with the lowest value of  $GD = 1.57$ .

For a fixed dimension  $K$ , "RLNC" strategy not surprisingly outperforms "R-XOR" and provides a really close bound to the capacity-achieving upper bound  $\mathcal{B}_{opt}^c$ . This is due to the fact that "RLNC" doesn't modify the degree distribution of RL packets contrary to "R-XOR".

The lower bounds  $\mathcal{B}$  of both coding strategies are improved with the increase of  $K$ . This is the consequence of two reasons. First, more encoded packets are combined together by the relays, increasing the packet diversity and thus reducing decoding time. Second, the size of the decoding overhead gets more and more negligible compared to  $K$ . However, you can not increase  $K$  infinitely because of the coefficient overhead that gets prohibitively high and the induced buffer size.

## VII. CONCLUSION

This paper has presented a flexible framework for evaluating the performance of simple wireless relay networks with respect to important performance criteria. Our model leverages the broadcast nature of wireless communications and accounts for interference. This framework allows for the determination of lower and upper Pareto bounds and their corresponding

TABLE IV  
PATH ANALYSIS FOR CAPACITY, DELAY AND ENERGY CRITERIA FOR THE 2-RELAY TOPOLOGY

Path	Path success probability
S-D	$\tau_S^1 p_{SD}^1$
S-A-D	$\tau_S^1 Q_{SA}^{12} p_{AD}^2$
S-B-D	$\tau_S^1 Q_{SB}^{13} p_{BD}^3$
S-A-B-A-D	$\tau_S^1 Q_{SA}^{12} (Q_{AB}^{23} Q_{BA}^{32}) p_{BD}^3$
S-B-A-B-D	$\tau_S^1 Q_{SB}^{13} (Q_{AB}^{23} Q_{BA}^{32}) p_{BD}^3$
:	:

Path	Delay per path
S-D	$\tau_S^1 p_{SD}^1$
S-A-D	$2\tau_S^1 Q_{SA}^{12} p_{AD}^2$
S-B-D	$2\tau_S^1 Q_{SB}^{13} p_{BD}^3$
S-A-B-A-D	$4\tau_S^1 Q_{SA}^{12} (Q_{AB}^{23} Q_{BA}^{32}) p_{AD}^2$
S-B-A-B-D	$4\tau_S^1 Q_{SB}^{13} (Q_{AB}^{23} Q_{BA}^{32}) p_{BD}^3$
:	:

Path	Energy per path
S-D	0
S-A-D	$\tau_S^1 Q_{SA}^{12}$
S-B-D	$\tau_S^1 Q_{SB}^{13}$
S-A-B-A-D	$\tau_S^1 Q_{SA}^{12} (Q_{AB}^{23} Q_{BA}^{32})$
S-B-A-B-D	$\tau_S^1 Q_{SB}^{13} (Q_{AB}^{23} Q_{BA}^{32})$
:	:

Pareto solutions. Network model and bounds for 1-relay and 2-relay networks have been assessed through simulations. We have shown that the upper MO bound provides a tight bound on the performance of network coding strategies. Thus, this work not only confirms the quality of our optimal upper Pareto bound, but also proposes a way of approaching it as close as wanted. We have even shown on these basic 2-relay cases that for such a broadcast forwarding paradigm, the combination of network coding and loops in the network outperforms classical non-loop forwarding strategies. This work will be extended to tackle problems where more relays and several flows transit in the network.

#### APPENDIX

This Appendix details the derivation of  $f_C$  in Eq. (14),  $f_D$  Eq. (15) and  $f_E$  in Eq. (16) for the 2-relay cases.

##### A. Capacity criterion $f_C$

$f_C$  is defined as the average number of packets received by the destination per packet sent by  $S$ . It is derived by adding the success probabilities of a packet arriving at  $D$  through all possible path. For example, for the direct path  $S - D$ , the success probability equals  $\tau_S^1 p_{SD}^1$ . For the relay path  $S - A - D$ , the capacity equals to  $\tau_S^1 Q_{SA}^{12} p_{AD}^2$ . Similarly, the success probability for other paths can be derived as shown in Table IV-left.

The sum of the success probabilities for all paths is the sum of the terms of the following infinite geometric series:

$$f_C = \tau_S^1 p_{SD}^1 + \tau_S^1 (E + F) (1 + Q_{AB}^{23} Q_{BA}^{32} + (Q_{AB}^{23} Q_{BA}^{32})^2 + Q_{AB}^{23} Q_{BA}^{32})^3 + \dots + (Q_{AB}^{23} Q_{BA}^{32})^n$$

with  $E = (Q_{SA}^{12} + Q_{SB}^{13} Q_{BA}^{32}) p_{AD}^2$  and  $F = (Q_{SB}^{13} + Q_{SA}^{12} Q_{AB}^{23}) p_{BD}^3$ . Here,  $\tau_S^1 (E + F)$  is the first term of the series, and  $Q_{AB}^{23} Q_{BA}^{32}$  is the common ratio. As  $n$  goes to infinity, the absolute value of  $Q_{AB}^{23} Q_{BA}^{32}$  must be less than one for the series to converge. This is true since we add the constraint  $Q_{AB}^{23} \leq 1 - \Delta$  and  $Q_{BA}^{32} \leq 1 - \Delta$  ( $\Delta = 0.05$ ) in our MO problem. The sum then becomes the criterion of Eq. (14).

##### B. Delay criterion $f_D$

$f_D$  is defined as the average delay a packet sent by the source needs to reach the destination. It is calculated by summing the delays for all packets arriving through all possible paths and dividing the result by the number of copies  $f_C$ . A similar path analysis is done for the delay computation in Table IV-middle. For example, for the direct path  $S - D$ , the

packet arrives in  $D$  in one hop and the corresponding delay equals  $f_{SD} = \tau_S^1 p_{SD}^1$ . For the relay path  $S - A - D$ , the packet takes two hops to arrive at  $D$  and thus the delay of the path equals to  $f_{SAD} = 2\tau_S^1 Q_{SA}^{12} p_{AD}^2$ . The infinite sum of the delays of Table IV is performed and provides the delay criterion of Eq. (15). Again it originates from the summation of the terms of an infinite series.

##### C. Energy criterion $f_E$

$f_E$  is defined as the average number of emissions done by all nodes per packet sent. It is derived by summing the probability for a relays to emit a packet per path and the probability for the source to emit a packet (which is equal to its rate  $\tau_S^1$ ). Similarly, the energy consumed per paths is shown in Table IV-right for all possible paths. Again, the summation of the terms of an infinite geometric series leads to the criterion of Eq. (16).

#### REFERENCES

- [1] A. Goldsmith, M. Effros, R. Koetter, and M. Médard, "Beyond Shannon: The Quest for Fundamental Performance Limits of Wireless Ad Hoc Networks," *IEEE Communications Magazine*, pp. 2–12, May 2011.
- [2] J. Luo, C. Rosenberg, and A. Girard, "Engineering Wireless Mesh Networks: Joint Scheduling, Routing, Power Control and Rate Adaptation," in *IEEE/ACM Transaction in Networking*, vol. 8, no. 5, pp. 1387–1400, October 2010.
- [3] Perkins, C. and Belding-Royer, E. and Das S., "Ad hoc On-demand Distance Vector Routing," 2003, RFC 3561.
- [4] Avestimehr, A. S. and Diggavi, N. and Tse, D. N. C., "A Deterministic Approach to Wireless Relay Networks," *IEEE Transactions on Information Theory*, pp. 1872–1905, April 2011.
- [5] J. Gorce, R. Zhang, K. Jaffrès-Runser, and C. Goursaud, "Energy, latency and capacity trade-offs in wireless multi-hop networks," in *Proceedings of IEEE PIMRC 2010*, sept. 2010, pp. 2757–2762.
- [6] R. Zhang, J.-M. Gorce, R. Dong, and K. Jaffrès-Runser, "Energy efficiency of opportunistic routing with unreliable links," in *WCNC 2009*, IEEE, april 2009, pp. 1–6.
- [7] K. Jaffrès-Runser, M. R. Schurgot, C. Comaniciu, and J.-M. Gorce, "A multiobjective performance evaluation framework for routing in wireless ad hoc networks," in *WiOpt 2010*, may 2010, pp. 113–121.
- [8] A. Fraboulet, G. Chelius, and E. Fleury, "Worldsens: development and prototyping tools for application specific wireless sensors networks," ser. IPSN '07. New York, NY, USA: ACM, 2007, pp. 176–185.
- [9] K. Deb, A. Pratap, and T. Meyarivan, "A fast and elitist multiobjective genetic algorithm: NSGA-II," *Evolutionary Computation, IEEE Transactions on*, vol. 6, no. 2, pp. 182–197, April 2002.
- [10] D. J. C. MacKay, "Fountain codes," *IEE Communications*, vol. 152, pp. 1062–1068, 2005.
- [11] A. Apavatjirut, C. Goursaud, K. Jaffrès-Runser, C. Comaniciu, and J. Gorce, "Toward increasing packet diversity for relaying It fountain codes in wireless sensor networks," *IEEE Commun. Lett.*, vol. 15, no. 1, pp. 52–54, 2011.
- [12] T. Ho, M. Medard, R. Koetter, D. Karger, M. Effros, J. Shi, and B. Leong, "A random linear network coding approach to multicast," *Information Theory, IEEE Transactions on*, vol. 52, no. 10, pp. 4413–4430, oct. 2006.